Indian Journal of Chemical Technology
Vol. 27, September 2020, pp. 367-374

Influence of SnO_2 nanoinclusions on the structural and dielectric properties of (PVA–PEO)/SnO_2 nanocomposites

Shobhna Choudhary*[1], Priyanka Dhatarwal[2] & R J Sengwa[2]

[1]CSIR-National Institute of Science Communication and Information Resources, New Delhi 110 012, India

[2]Dielectric Research Laboratory, Department of Physics, Jai Narain Vyas University, Jodhpur 342 005, India

E-mail: shobhnachoudhary@rediffmail.com

Received 25 June 2020; accepted 25 August 2020

Nanofiller concentration dependent, tunable-type structural, dielectric, thermo-mechanical, and optical properties of the polymer nanocomposites (PNCs) have established them as technologically smart multifunctional materials for advances in stretchable and flexible-type organoelectronic, optoelectronic, and energy harvesting/storage devices. In this work, organic-inorganic hybrid PNC films comprising poly(vinyl alcohol) (PVA) and poly(ethylene oxide) (PEO) blend as host matrix (PVA–PEO; 50–50 wt%) dispersed with varying concentration of tin oxide (SnO_2) nanoparticles up to 5 wt% have been prepared by the solution-cast method. The influence of SnO_2 loading on the percent crystallinity of the host matrix and the structural parameters of the PEO crystallites has been examined by the X-ray diffraction (XRD) measurements of the PNC films. The results reveal that the percent crystallinity of the semicrystalline (PVA–PEO) matrix gradually enhanced, whereas the interlayer spacing, crystallite size, and interchain separation of the PEO crystallites varied anomalously with the increase of SnO_2 concentration in the PNC films. The complex dielectric permittivity, alternating current (ac) electrical conductivity, and electric modulus dispersion over the broad frequency range (20 Hz–1 MHz) of these (PVA–PEO)/SnO_2 films has been characterized by employing the dielectric relaxation spectroscopy (DRS). It has been observed that 1 wt% SnO_2 nanoinclusion abruptly reduced the interfacial, dipole polarizations, and also electrical conduction of the host matrix, whereas considerably enhanced hindrance to the PEO chain segmental motion studied at 30 °C. The temperature dependent study (30–60 °C) of the representative PNC film of 3 wt% nanofiller reveals its thermally activated non-linear dielectric polarization at fixed frequency and also Arrhenius behaviour of the dielectric relaxation processes of significantly low activation energy (≃ 0.14 eV). The structural, dielectric, and electrical properties of the (PVA–PEO)/SnO_2 films have been critically analyzed for their suitability as controllable low dielectric permittivity polymer nanodielectric (PNDs) materials for biodegradable electronic devices.

Keywords: Polymer nanocomposites, Dielectric properties, Electrical conductivity, Relaxation times, Activation energy, X-ray diffraction

Flexible and stretchable-type matrices of polymers and their blends are widely used with state-of-the-art inorganic/organic nanoinclusions to get polymer nanocomposites (PNCs) bearing integrated appealing properties of polymer and nanofiller for their advanced multifunctional technological applications[1–7]. For the confirmation of industrial suitability of the PNCs, their morphological, structural, thermal, mechanical, chemical, dielectric, electrical, and optical properties are characterized with an attempt to achieve these somehow tunable properties with nanofiller concentration in the host polymer matrix[1–10].

Characterization of dielectric and electrical parameters of the PNC materials and their possible tuning with nanofiller concentration realizes them as polymer nanodielectrics (PNDs) which are considered potential candidates in the design and development of a variety of electronic and electrical devices[1–12]. The behaviour of interfaces between the PNC constituents principally governs their dielectric polarization, losses, and structural dynamics[6–17]. So far, a variety of polymer matrices and nanofillers have been considered for achieving their technological desired dielectric properties as well as structural properties[6,7,13,17]. In the last decade, the authors have investigated a large number of promising PNC materials for their different technological applications[8–12,18–26]. In these studies, several polar polymers and their blend matrices with 2-D and 3-D nanofiller (metal and non-metal oxides, and montmorillonite (MMT) clay) were used to develop appropriate dielectric, optical, and structural properties PNCs.

Among the polar polymers, poly(vinyl alcohol) (PVA) and poly(ethylene oxide) (PEO) are

biodegradable, almost non-toxic, hydrophilic, and water soluble materials and their blends are mostly considered for the preparation of advanced PNC films with a variety of nanoinclusions[18–22,27–34]. The high optical transparency of PVA film and also good flexibility realizes it suitable for preparation of organoelectronic and optoelectronic materials[35,36], whereas, the high ability of PEO chain interactions with alkali metal salts have recognized this linear chain polymer as appealing matrix for the preparation of solid polymer electrolyte (SPE) films[37,38].

In recent years, the detailed structural, dielectric, and electrical properties of MMT clay nanoplatelets loaded (PVA–PEO)/MMT nanocomposites[18,19], silica (SiO_2) nanoparticles filled (PVA–PEO)/SiO_2 films[20], zinc oxide (ZnO) nanoparticles filled (PVA–PEO)/ZnO films[21], and alumina (Al_2O_3) nanoparticles filled (PVA–PEO)/Al_2O_3 films[22] have been investigated in our laboratory for their suitability as flexible-type nanodielectrics and optoelectronic materials. In continuation of these works on PVA–PEO blend matrix based PNCs, the present paper deals with structural, dielectric, and electrical properties and also the dielectric relaxation processes in the (PVA–PEO)/SnO_2 films for confirmation of their suitability as flexible and stretchable-type PNDs in regards to the biodegradable electronic device applications. Due to interesting electronic and optical properties of SnO_2[39], it has been frequently used for preparation of various technological useful PNC materials based on different types of polymer matrices[23,40–49].

Experimental Section

Materials

The PVA (M_w = 77×10^3 g mol^{-1}) of Loba Chemie, India, and PEO (M_w = 6×10^5 g mol^{-1}) and SnO_2 nanopowder (particles size < 50 nm) of Sigma-Aldrich were used as precursors for the preparation of (PVA–PEO)/SnO_2 films. The PVA–PEO blend matrix (50–50 wt%) dispersed with x wt% amounts of SnO_2 (x = 0, 1, 3 and 5 wt% with respect to weight of polymer blend) were prepared by solution-casting method. For preparation of each (PVA–PEO)/SnO_2 film, in the beginning, the same amounts of PVA and PEO were dissolved in deionized water in separate conical flasks, and then these polymer solutions were mixed and stirred with magnetic bar to get appropriate PVA–PEO blend solution. The required amount of SnO_2 for its x wt% was firstly dispersed in the deionized water and after that, it was mixed with polymer blend solution. A homogenous (PVA–PEO)/x wt% SnO_2 viscous solution was obtained through ultrasonication and magnetic stirring. This solution was cast on to a poly propylene dish and was dried at room temperature which resulted free standing PNC film. All the PNC films for different concentrations of SnO_2 in the PVA–PEO blend were prepared by adopting the same steps as mentioned above and finally these films were vacuum dried. The thicknesses of (PVA–PEO)/SnO_2 films were found in the range 0.22 to 0.26 mm.

Measurements

The structural characterization of (PVA–PEO)/SnO_2 films were made from their XRD patterns which were recorded in reflection mode at the scan rate 3°/min. A PANalytical X′pert Pro MPD diffractometer of Cu-Kα radiation (wavelength λ = 0.15406 nm) was operated at 45 kV and 40 mA for recording the XRD patterns of the films. The dielectric and electrical measurements of these PNC films were carried out over the frequency range from 20 Hz to 1 MHz using an Agilent technologies 4284A precision LCR meter equipped with circular plates 16451B solid dielectric test fixture. The details about measurements and determination of frequency dependent dielectric and electrical functions are the same as reported elsewhere[9,21,22].

Results and Discussion

Structural analysis

The XRD traces of (PVA–PEO)/SnO_2 films are depicted in Fig. 1. It can be noted from Fig. 1a that the pristine PVA–PEO blend film (i.e., x = 0) exhibits nearly equal intensities diffraction peaks at 2θ = 19.54° and 23.66° which are found close to the diffraction peaks positions of pristine PEO film[8,19] confirming the presence of PEO crystallites in the blend. Further, the intensities of both these peaks of the PVA–PEO blend are about half as compared to that of the pristine PEO film[8] which reveals that the PEO crystallites reduced when it is blended with the PVA in equal weight amounts favouring the earlier findings[19–22]. When SnO_2 nanoparticles were dispersed in the PVA–PEO blend matrix, several alterations in the XRD patterns of the (PVA–PEO)/SnO_2 films appeared as compared to the host polymer matrix. Fig. 1a confirms that the peaks positions slightly changed but there was huge variation in the intensities of these PEO peaks reflecting some

alteration in percent crystallinity of the host blend film. The SnO_2 peaks are also exhibited in these PNC films and their intensities enhanced with the increase of nanofiller concentration (see Fig. 1b). Almost linear increase of SnO_2 peak intensity (I_{110}) is found (see Fig. 1c), which evidences homogeneous dispersion of the loaded nanoparticles in the polymer matrix[47,48] and the PNC films formation is of good quality from the nanotechnology point of view.

The percent crystallinity of the PVA–PEO matrix X_c in these PNC films was determined using the relations $X_c\,(\%) = (A_c/(A_c+A_a))\times 100$ [25,47]. In this relation A_c and A_a are respectively the areas of crystalline peaks and the amorphous hump in the XRD traces considered from 10° to 25°) and these areas were computed using the OriginPro® software. From Fig. 1c, it can be noted that the plot of X_c versus x (wt%) of nanofiller for these PNC materials is linear which evidence that in the presence of SnO_2 nanoparticles there is growth in crystallites of the films.

The structural properties of these PNC materials were analyzed in-depth by determining the interlayer spacing d, crystal size L, and interchain separation R of the PEO crystallites corresponding to its both the peaks (~19.5° and ~23.6°) using the relations demonstrated elsewhere[50]. From Fig. 1c, it can be seen that the d and R values change slightly but there is large alteration in the L values with the increase of SnO_2 concentration in these PNC films. Further, all these structural parameters (d, L, and R) vary anomalously with increasing SnO_2 concentration in the PVA–PEO matrix.

Dielectric dispersion and dynamical relaxation

Figure 2 depicts the complex dielectric permittivity (ε′, ε″), and dielectric loss tangent (tanδ) versus frequency plots for the (PVA–PEO)/SnO_2 films at 30 °C, and also at 30, 40, 50, and 60 °C for the 3 wt% SnO_2 nanoincluded PNC film. This figure evidences that ε′, ε″, and tanδ values of these PNC films (x = 1, 3, and 5 wt%) at all the frequencies ranging from 20 Hz to 1 MHz are significantly lower than that of the host PVA–PEO blend matrix (x = 0) which confirms that the dielectric polarization of the host polymer matrix decreased by the inclusion of SnO_2 nanoparticles, although the SnO_2 dielectric constant[51] is much higher than this polymer matrix. Further, it can also be noted from Fig. 2a that the decrease in ε′ values is relatively fast and linear at lower frequencies, slightly slow and non-linear in the intermediate frequencies, and slowest but linear in the higher frequencies. The ε′ values of a dielectric material is the measure of its polarization strength, and the frequency dependent dispersion behaviour of ε′ values attribute to the different polarization processes in these heterogeneous composite material under the influence of ac electric field. In the experimental frequency range (i.e., 20 Hz to 1 MHz),

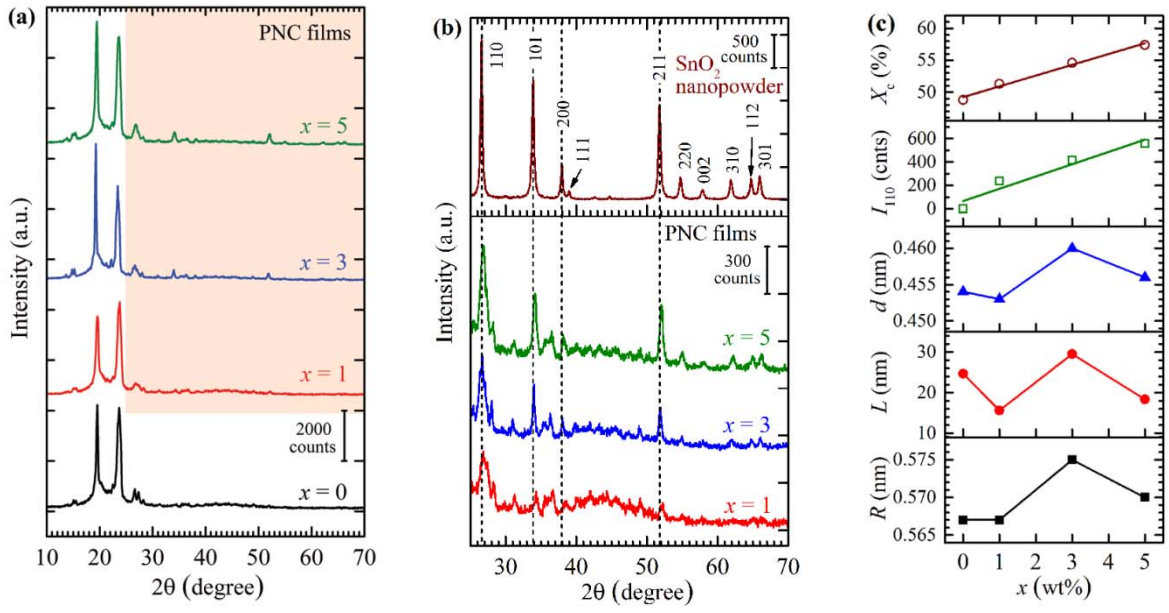

Fig. 1 — XRD patterns of (a) (PVA–PEO)/x wt% SnO_2 films (x = 0, 1, 3, and 5), (b) the SnO_2 nanopowder and the enlarged view of SnO_2 peaks in PNC films, and (c) the plots of X_c, I_{110}, d, L, and R versus varying SnO_2 concentrations x (wt%) of the PNC films.

most of the PNCs exhibit interfacial polarization (IP) at lower frequencies and the dipolar polarization (DP) at higher frequencies, and the starting and end frequency range of these polarizations depend on the constituents and their relative amounts in the hybrid composites[6,8–12,16,20–26,47,48]. Further, the IP-process attribute to the charge storage at the interfaces of different constituents in the PNCs and the DP-process is an evidence of dipole ordering of the polar molecules[9,10,12,14]. In the semicrystalline (PVA–PEO)/SnO_2 materials, there are interfaces of crystalline and amorphous phases of the polymers and also their interfaces with the nanoparticles of the filler. The $\varepsilon'(f)$ dispersion confirms that there is decrease in both the polarization processes with increase of frequency but the IP-process reduces relatively more as compared to the DP-process of the PVA–PEO structures in the presence of loaded SnO_2 nanoparticles.

The $\varepsilon''(f)$ and $\tan\delta(f)$ spectra of these PNC materials exhibited relaxation peak in the intermediate frequency range (see Fig. 2a) which can be assigned to the chain segmental motion of PEO structures because of the fact that the pristine PEO display relaxation peak in this frequency range at room temperature[8]. In comparison to the relaxation peak frequency of the PVA–PEO blend film these PNCs peaks are appeared at lower frequencies. Further, these peaks are exhibited sharp in the tanδ spectra in contrast to that of the ε'' spectra. The relaxation times designated as τ_ε and τ_s for these PNC materials were determined from the peak frequency f_p values of ε'' and tanδ peak, respectively using the relation $\tau_s = 1/2\pi f_p$, and it was noted that there is higher τ_ε and τ_s of the PNC films in comparison to that of the host matrix confirming that the SnO_2 nanoparticles increase the hindrance to the PEO chain segmental motion. These relaxation times of the PNC materials are discussed in detail in the next section.

Thermal effect on the dielectric polarization and relaxation processes of these PNC materials has been examined by dielectric measurements of 3 wt% SnO_2 dispersed PNC film (intermediate concentration of nanofiller) as a representative sample at various

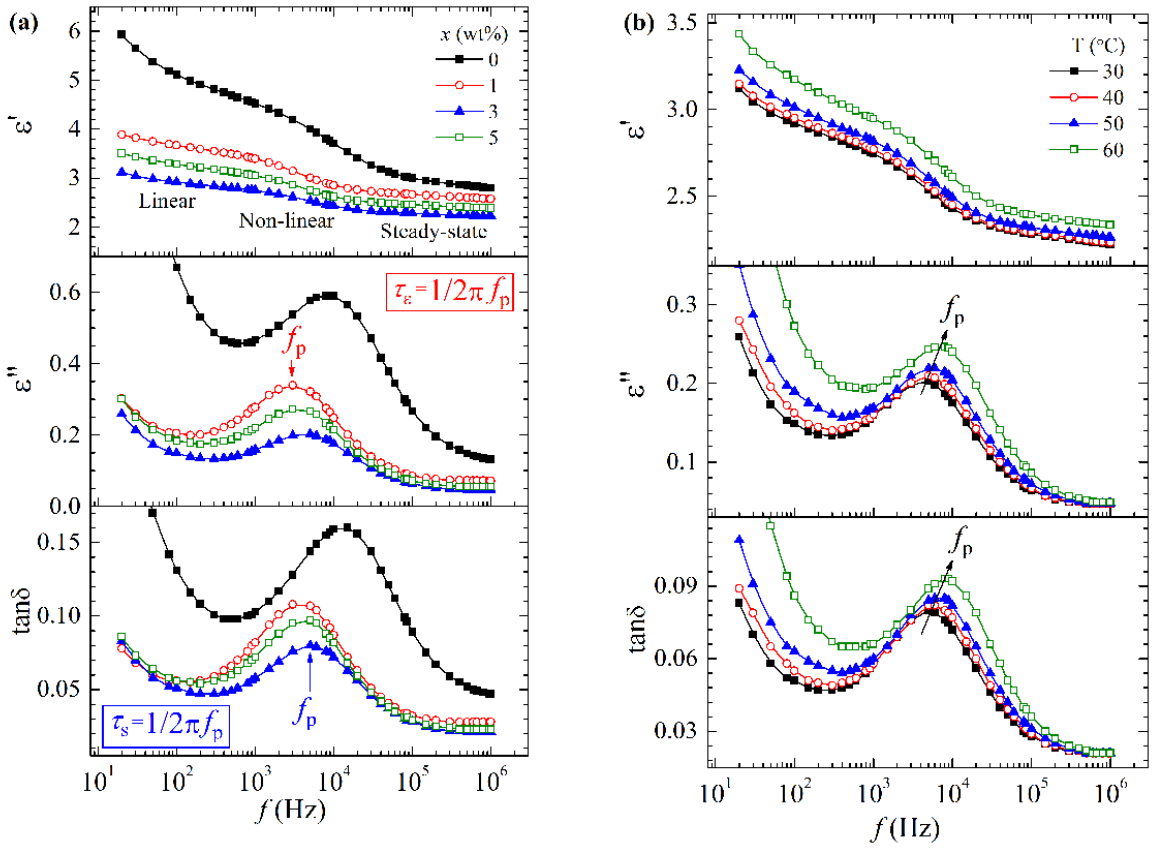

Fig. 2 — Frequency dependent real part ε' and loss part ε'' of complex dielectric permittivity, and loss tangent tanδ of (a) (PVA–PEO)/*x* wt% SnO_2 films (*x* = 0, 1, 3, and 5) at 30 °C, and (b) (PVA–PEO)/3 wt% SnO_2 film at different temperatures.

temperatures. Fig. 2b explains that the ε′ values moderately increase when the temperature of the PNC film increases in steps of 10 °C from 30 to 60 °C. Furthermore, the relaxation peaks of ε″ and tan δ spectra have a gradual shift towards higher frequencies with enhanced intensity (marked with arrows in the figure) when the temperature of the film increases. These temperature dependent dielectric results evidence thermally activated dielectric polarization and relaxation behaviour of the (PVA–PEO)/SnO_2 film which is in agreement of several other PNC materials[8–10,20–22].

Figure 3 depicts the variation of ε′ against x (wt%) of nanofiller for the PNC films, and also the ε′ against temperature T (°C) of the 3 wt% SnO_2 included PNC film at different fixed frequencies. One can see from Fig. 3a that the ε′ values of these PNC decreased largely at 1 wt% SnO_2 loading and then reaches

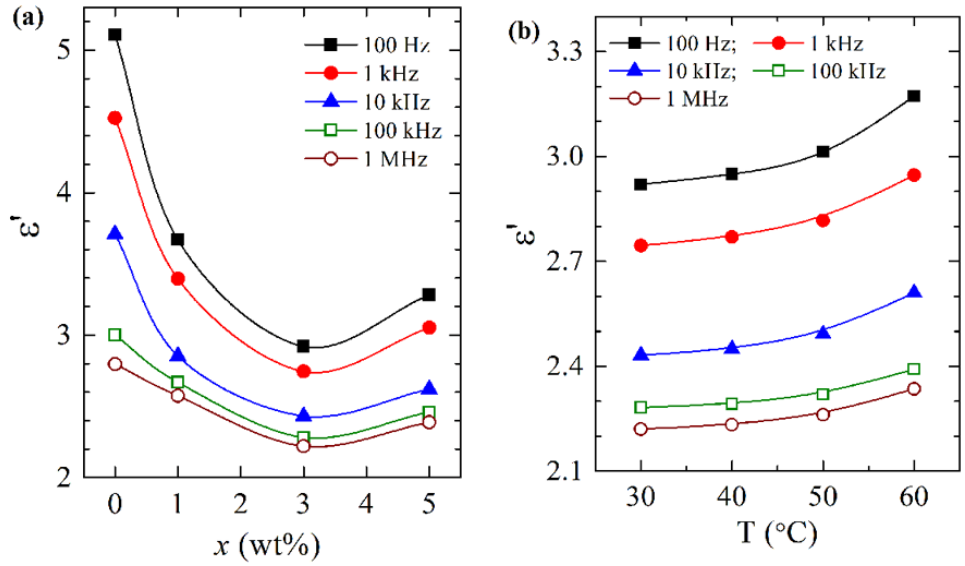

Fig. 3 — (a) SnO_2 concentration dependent values of ε′ for (PVA–PEO)/x wt% SnO_2 films (x = 0, 1, 3, and 5) at 30 °C and (b) temperature dependent ε′ values of (PVA–PEO)/3 wt% SnO_2 film at various frequencies.

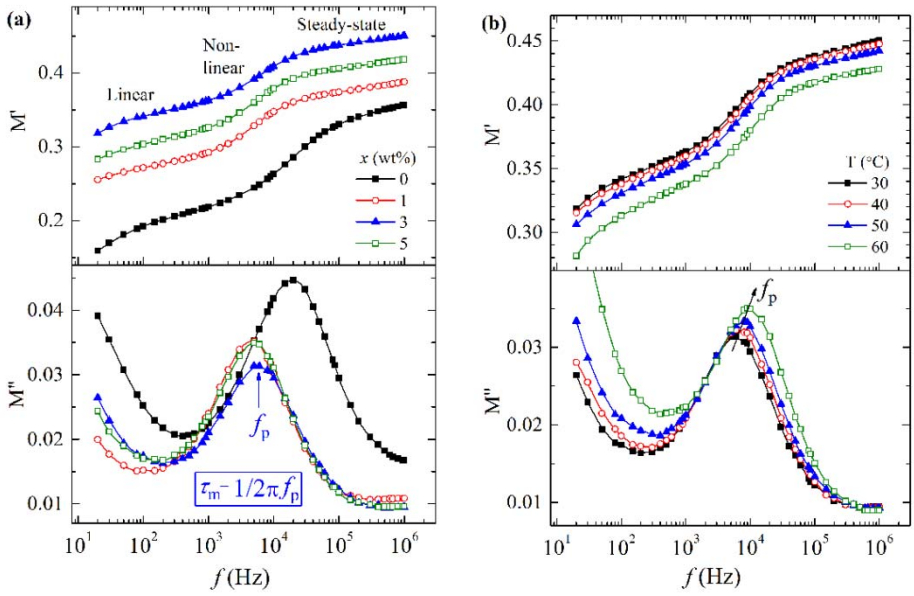

Fig. 4 — Frequency dependent real part M' and loss part M'' of complex electric modulus of (a) (PVA–PEO)/x wt% SnO_2 films (x = 0, 1, 3, and 5) at 30 °C, and (b) (PVA–PEO)/3 wt% SnO_2 film at different temperatures.

minimum at 3 wt% and after that slightly increase at 5 wt% at all the fixed frequencies. This finding evidences that the dielectric permittivity can be considerably tuned by keeping low amount of the SnO_2 nanofiller. Fig. 3b explains that there is a non-linear increase in ε′ values of the PNC film at all the fixed frequencies with the increase of film temperature. Further, the non-linearity is relatively high at low frequencies (IP-process region) as compared to that of the higher frequencies (DP-process region) of the thermally activated PNC film.

Electric modulus and conductivity relaxation

Electric modulus (*M′* and *M″*) spectra of the (PVA–PEO)/SnO_2 films at a fixed temperature are depicted in Fig. 4a, whereas for 3 wt% SnO_2 loaded PNC film at different temperatures are depicted in Fig. 4b. A step-like shape of *M′* spectra observed for these PNC materials is in agreement with the results of different PNCs demonstrated earlier[8,9,12,26,52,53]. As compared to the shapes and positions of tanδ relaxation peaks (see Fig. 2), the *M″* spectra exhibit relatively intense relaxation peaks (see Fig. 4) which have also appeared at slightly higher frequencies. The order of peak frequencies for these PNC films in their different functions is $f_{p(M'')} > f_{p(\tan\delta)} > f_{p(\varepsilon'')}$. Many PNCs also exhibited similar order of these relaxation peak frequencies which is expected because several unwanted effects contributing in dielectric polarization are principally eliminated in the electric modulus formalism[8–10,18,22,37]. The electric modulus relaxation time τ_m which is commonly called conductivity relaxation denoted by τ_σ is determined from the relaxation peak frequency of *M″* spectra.

Figure 5 shows the plots of various relaxation times (τ_ε, τ_s, and τ_m) versus *x* wt% SnO_2 for the PNC films at 30 °C and also against 1000/*T* for the PNC film containing 3 wt% SnO_2. Fig. 5a reveals that the trend of variation in τ_ε, τ_s, and τ_m against *x* (wt%) of nanofiller are identical for the (PVA–PEO)/SnO_2 films. Furthermore, all these PNC films have higher relaxation times as compared to their host PVA–PEO film, and the alteration with nanofiller concentration from 1 to 5 wt% is found insignifiant. The temperature dependent values of all these relaxation times of the (PVA–PEO)/3 wt% SnO_2 film exhibited Arrhenius behaviour of nearly same activation energies ($E_\tau \simeq 0.14$ eV). The low E_τ values confirm that the dynamical processes in the composite material are fast and occurring in identical manner up to 5 wt% SnO_2 loading.

AC electrical conductivity

Figure 6 demonstrates the frequency dependent real part of ac electrical conductivity σ′ of the (PVA–PEO)/SnO_2 films. These plots are non-linear in the frequency range 20 Hz to 1 MHz which is due to semicrystalline nature of the PNC films demonstrated

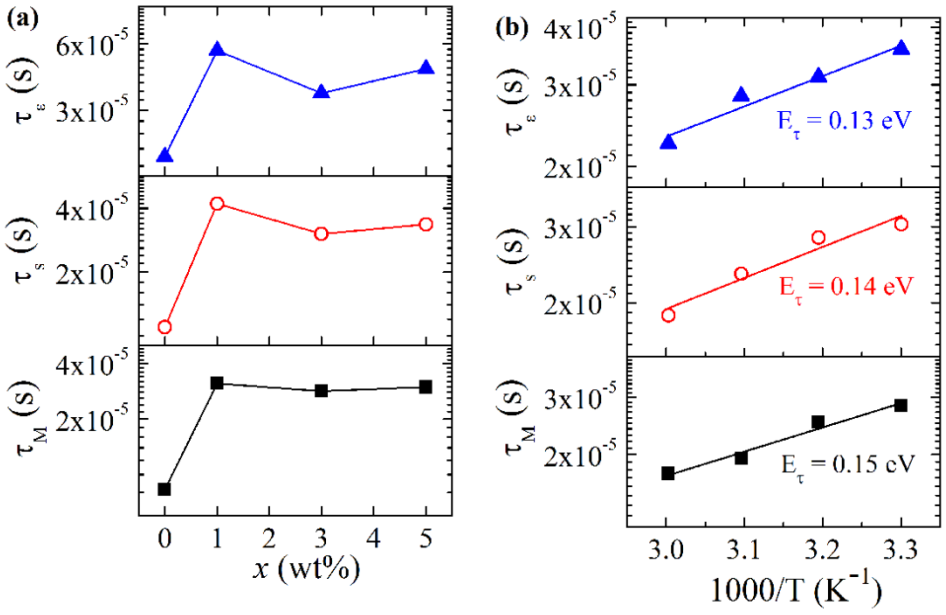

Fig. 5 — (a) SnO_2 concentration dependent relaxation times τ_ε, τ_s and τ_M of (PVA–PEO)/*x* wt% SnO_2 films (*x* = 0, 1, 3, and 5) at 30 °C and (b) Arrhenius behaviour of relaxation times of (PVA–PEO)/3 wt% SnO_2 film.

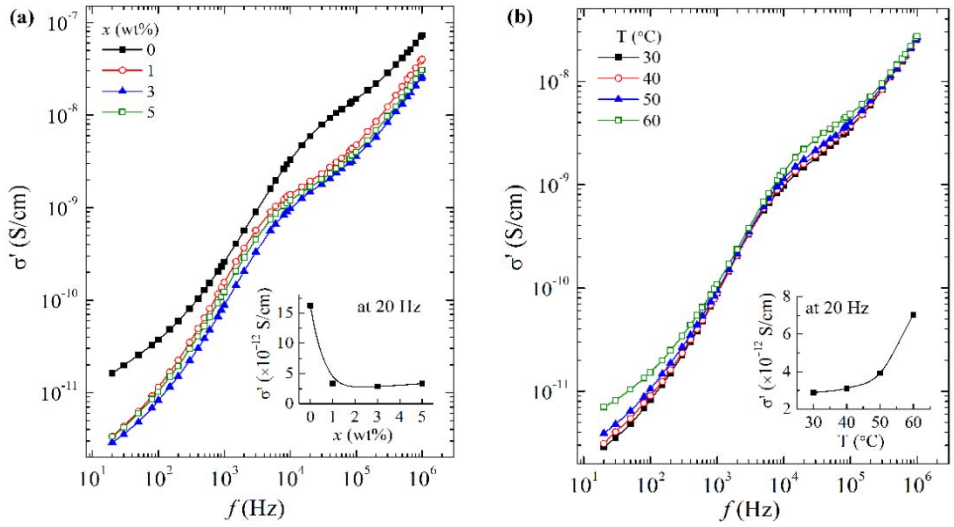

Fig. 6 — Frequency dependent real part σ′ of (a) (PVA–PEO)/*x* wt% SnO_2 films (*x* = 0, 1, 3, and 5) at 30 °C, and (b) (PVA–PEO)/3 wt% SnO_2 film at different temperatures. The insets present σ′ values at 20 Hz versus varying SnO_2 concentrations *x* (wt%) and different temperatures

earlier[8,12,18,21]. Further, the σ′ values of these PNC films are found significantly low as compared to that of their PVA–PEO host matrix. One can see from the inset of the host matrix that the further changes in σ′ values with increase of SnO_2 concentration are insignificant at fixed frequency (20 Hz). The decreased σ′ of these PNC films confirms their suitability as appropriate electrical insulators in the development of biodegradable microelectronic devices. One can note that the effect of temperature on the σ′ values at low frequencies is significant for the temperature dependent studied PNC film containing 3 wt% SnO_2. It can be noted from the inset of Fig. 6b that the increase of σ′ at 20 Hz of the PNC film is about half an order with the increase of temperature from 30 to 60 °C which reveal the temperature tunable σ′ of the film at low frequencies.

Conclusions

This paper reports the detailed structural, dielectric and electrical properties, and the dielectric relaxation processes of the (PVA–PEO)/SnO_2 films over the frequency range from 20 Hz to 1 MHz at 30 °C, and also 3 wt% SnO_2 containing PNC film at various temperatures in the range 30–60 °C. The loading of SnO_2 nanoparticles reduced the complex dielectric permittivity and ac electrical conductivity, and increased hindrance to the structural dynamics of the PNC films. Results revealed that the dispersion of 1 and 3 wt% SnO_2 nanoparticles in the PVA–PEO blend matrix reduced the dielectric permittivity values which can be tuned. Further, the ac electrical conductivity can be reasonably reduced with small dispersion of SnO_2 nanoparticles. The PNC film exhibits the thermally activated dielectric polarization and significantly low activation energy of the relaxation processes. The SnO_2 nanoinclusions increase the percent crystallinity of the PNC films host matrix but the PEO crystals parameters anomalously changes with the increase of SnO_2 concentration. This dielectric study evidences the suitability of these (PVA–PEO)/SnO_2 films as low permittivity tunable biodegradable PNDs.

Acknowledgements

One of the authors (PD) thanks the CSIR, New Delhi for the award of a postdoctoral research associate fellowship.

References

1 Gupta R K, Kennel E & Kim K J, Polymer Nanocomposites Handbook. CRC Press, (Boca Raton), 2009.
2 Ponnamma D, Sadasivuni K K, Cabibihan J J & Al-Maadeed M A A, Smart Polymer Nanocomposites: Energy Harvesting, Self-Healing and Shape Memory Applications. Springer International Publishing, (Switzerland), 2017.
3 Guo J G, Song K & Liu C, Polymer-based Multifunctional Nanocomposites and their Applications. Elsevier Inc., (Amsterdam), 2019.
4 Pielichowski K & Majka T, Polymer Composites with Functionalized Nanoparticles, Elsevier Inc., (Amsterdam), 2019.
5 Huang X & Zhi C, Polymer Nanocomposites: Electrical and Thermal Properties. Springer International Publishing, (Switzerland), 2016.

6 Tanaka T & Vaughan A S, Tailoring of Nanocomposite Dielectrics: From Fundamentals to Devices and Applications. Temasek Boulevard, Pan Stanford Publishing Pte. Ltd., (Singapore), 2017.
7 Zhong W H & Li B, Polymer Nanocomposites for Dielectrics. CRC Press, Taylor & Francis Group, Pan Stanford Publishing Pte. Ltd., (New York), 2017.
8 Sengwa R J & Choudhary S, *J Alloys Compd*, 701 (2017) 652.
9 Sengwa R J & Choudhary S, *Curr Appl Phys*, 18 (2018) 1041.
10 Sengwa R J, Choudhary S & Dhatarwal P, *J Mater Sci Mater Electron*, 30 (2019) 12275.
11 Dhatarwal P & Sengwa R J, *J Polym Res*, 26 (2019) 196.
12 Dhatarwal P & Sengwa R J, *Mater Res Bull*, 129 (2020) 110901.
13 Tan D Q, *Adv Func Mater*, 30 (2020) 1808567.
14 Mao F, Shi Z, Wang J, Zhang C, Yang C & Huang M, *Adv Compos Hybrid Mater*, 1 (2018) 548.
15 Stavropoulos S G, Sanida A & Psarras G C, *Exp Polym Lett*, 14 (2020) 477.
16 Lin Y, Hu S & Wu G, *J Phys Chem C*, 123 (2019) 6616.
17 Anandraj J & Joshi G M, *Compos Interfaces*, 25 (2018) 455.
18 Sengwa R J, Choudhary S & Sankhla S, *Comps Sci Technol*, 70 (2010) 1621.
19 Sengwa R J & Choudhary S, *J Appl Polym Sci*, 131 (2014) 40617.
20 Choudhary S, *Indian J Eng Mater Sci*, 23 (2016) 399.
21 Choudhary S, *Physica B*, 522 (2017) 48.
22 Choudhary S, *Indian J Chem Technol*, 25 (2018) 51.
23 Sengwa R J, Dhatarwal P & Choudhary S, *Mater Today Commun*, 25 (2020) 101380.
24 Choudhary S, Dhatarwal P & Sengwa R J, *Indian J Chem Technol*, 27 (2020) 201.
25 Sengwa R J, Choudhary S & Dhatarwal P, *Adv Compos Hybrid Mater*, 2 (2019) 162.
26 Choudhary S, *J Phys Chem Solids*, 121 (2018) 196.
27 Elashmawi I S, Abdelrazek E M, Hezma A M & Rajeh A, *Physica B Condens Matter*, 434 (2014) 57.
28 Aziz S B, Abdullah O Gh, Hussein A M, Abdulwahid R T, Rasheed M A, Ahmed H M, Abdalqadir S W & Mohammed A R, *J Mater Sci Mater Electron*, 28 (2017) 7473.
29 Ragab H M, *Results Phys*, 7 (2017) 2057.
30 Farea M O, Abdelghany A M, Meikhail M S & Oraby A H, *J Mater Res Technol*, 9 (2020) 1530.
31 Xu L, Wei K, Cao Y, Ma S, Li J, Zhao Y, Cui Y & Y Cui, *RSC Adv*, 10 (2020) 5462.
32 He M, Chen M, Dou Y, Ding J, Yue H, Yin G, Chen X & Cui Y, *Polymers*, 12 (2020) 305.
33 Hadi A, Hashim A & Al-Khafaji Y, *Trans Electr Electron Mater*, 21 (2020) 283.
34 Hashim A, Al-Khafaji Y & Hadi A, *Trans Electr Electron Mater*, 20 (2019) 530.
35 Deshmukh K, Ahamed M B, Deshmukh R R, Pasha S K K, Sadasivuni K K, Ponnamma D & Chidambaram K, *Eur Polym J,* 76 (2016) 14.
36 Halder M, Das A K & Meikap A K, *Mater Res Bull*, 104 (2018) 179.
37 Choudhary S & Sengwa R J, *Mater Chem Phys*, 142 (2013) 172.
38 Arya A & Sharma A L, *J Phys D Appl Phys*, 50 (2017) 443002.
39 Orlandi M O, Tin Oxide Materials: Synthesis, Properties, and Applications, Elsevier Inc. (Amsterdam), 2020.
40 Jian K S, Chang C J, Wu J J, Chang Y C, Tsay C Y, Chen J H, Horng T L, Lee G J, Karuppasamy L, Anandan S & Chen C Y, *Polymers*, 11 (2019) 184.
41 Senthil S, Srinivasan S, Thangeeswari T & Ratchagar V, *J Mater Sci Mater Electron*, 30 (2019) 19841.
42 Sarkar P K, Bhattacharjee S, Prajapat M & Roy S, *RSC Adv*, 5 (2015) 105661.
43 Kar E, Bose N, Dutta B, Banerjee S, Mukherjee N & Mukherjee S, *Energy Convers Manag*, 184 (2019) 600.
44 Reddy Channu V S, Rambabu B, Kumari K, Kalluru R R & Holze R, *Electrochim Energy Technol*, 4 (2018) 32.
45 Choudhary S, *Compos Commun*, 5 (2017) 54.
46 Peng T, Wen Y, Wang C, Wang Y, Zhang G, Zhang Y & Dionysiou D D, *Mater Sci Semicond Process*, 102 (2019) 104586.
47 Dhatarwal P, Choudhary S & Sengwa R J, *Mater Lett*, 273 (2020) 127913.
48 Dhatarwal P, Choudhary S & Sengwa R J, *Polym Bull*, (2020) DOI: https://doi.org/10.1007/s00289-020-03215-2.
49 Choudhary S & Sengwa R J, *Electrochim Acta*, 247 (2017) 924.
50 Sengwa R J & Dhatarwal P, *Electrochim Acta*, 338 (2020) 135890.
51 Azam A, Ahmed A S, Chaman M & Naqvi A H, *J Appl Phys*, 108 (2010) 094329.
52 Tsonos C, Zois H, Kanapitsas A, Soin N, Siores E, Peppas G D, Pyrgioti E C, Sanida A, Stavropoulos S G & Psarras G C, *J Phys Chem Solids*, 129(2019) 378.
53 Abutaliba M M & Rajeh A, *Phys B Condens Matter*, 578 (2020) 411796.